Probing Phenylalanine/Adenine π-Stacking Interactions in Protein Complexes with Explicitly Correlated and CCSD(T) Computations

Kari L. Copeland,[†] Julie A. Anderson,[†] Adam R. Farley,[‡] James R. Cox,[‡] and Gregory S. Tschumper*,[†]

Department of Chemistry and Biochemistry, University of Mississippi, University, Mississippi 38677, and Department of Chemistry, Murray State University, Murray, Kentucky 42071

Received: June 23, 2008; Revised Manuscript Received: September 4, 2008

To examine the effects of π-stacking interactions between aromatic amino acid side chains and adenine bearing ligands in crystalline protein structures, 26 toluene/(N9-methyl)adenine model configurations have been constructed from protein/ligand crystal structures. Full geometry optimizations with the MP2 method cause the 26 crystal structures to collapse to six unique structures. The complete basis set (CBS) limit of the CCSD(T) interaction energies has been determined for all 32 structures by combining explicitly correlated MP2-R12 computations with a correction for higher-order correlation effects from CCSD(T) calculations. The CCSD(T) CBS limit interaction energies of the 26 crystal structures range from -3.19 to -6.77 kcal mol^{-1} and average -5.01 kcal mol^{-1}. The CCSD(T) CBS limit interaction energies of the optimized complexes increase by roughly 1.5 kcal mol^{-1} on average to -6.54 kcal mol^{-1} (ranging from -5.93 to -7.05 kcal mol^{-1}). Corrections for higher-order correlation effects are extremely important for both sets of structures and are responsible for the modest increase in the interaction energy after optimization. The MP2 method overbinds the crystal structures by 2.31 kcal mol^{-1} on average compared to 4.50 kcal mol^{-1} for the optimized structures.

1. Introduction

Noncovalent interactions substantially influence nearly every type of biological process. Among these are an important class of dispersion interactions known as π-stacking interactions. Proteins and nucleic acids strongly rely upon π-type interactions as determinants of their basic structure and function.[1−3] For example, π-stacking interactions such as those of nucleic acid bases and aromatic hydrocarbons play crucial roles in DNA base pair assembly and protein folding.[4] In addition to their immense importance to biochemistry, these interactions contribute to many areas of medicinal chemistry such as in the reactivity of drugs[5] and to areas of nanotechnology such as in the production of electronic devices.[6]

Given their preeminence in the areas of chemistry and biology, π-interactions have been the focus of many experimental and theoretical investigations.[7−25] One of the most interesting cases is the propensity for π-interactions to influence the alignment of aromatic groups in the crystalline state of proteins.[26] To examine the effects of π-interactions in proteins with electronic structure computations, researchers use small prototypes to model the energetics of large biological systems. The benzene dimer has been the most widely studied model for aromatic π-stacking interactions[8,13,16,18,19,21,27] and has provided much insight into the nature of delocalized π-interactions.

Nature, however, is replete with N-substituted aromatic systems (e.g., nucleic acid bases) as is the field of supramolecular chemistry (e.g., 1,3,5-triazine).[28] Adenine-bearing ligands contribute to a vast majority of these complexes such as in adenosine 5′-triphosphate (ATP),[29,30] nicotinamide adenine dinucleotide phosphate ($NADP^+$), and flavin adenine dinucleotide (FAD) interactions.[31] While the role of π-stacking interactions between nucleic acid base dimers has been widely studied,[4,9−11,17,23,32−35] the stacking interactions between these nucleic acid bases and aromatic amino acid residues in proteins have not been characterized as thoroughly.

Models of these interactions range from simple prototypes such as pyridine/toluene[14] and triazine/benzene[25] to mixed dimers composed of adenine and aromatic amino acid residues such as phenylalanine (Phe). A few notable examples of the latter include the work of Mao et al. in which adenosine 5′-triphosphate (ATP) recognition in 68 adenylate−binding protein complexes was studied by pairing the adenine base with multiple residues including lysine, arginine, phenylalanine, tryptophan, and tyrosine.[30] This work, which was done at the MP2/6-311+G* level of theory, identified and analyzed three classes of binding interactions (hydrogen bonding, π-stacking interactions, and cation π-interactions) as significant contributors to the overall binding of ATP in proteins. The effects of geometry and protonation state were investigated in histidine−aromatic complexes (i.e., histidine interacting with phenylalanine, tyrosine, tryptophan, or adenine in gas phase, water, and protein-like environments) by Cauët et al.[36] MP2 computations with a specialized 6-31G(2d(0.8,0.2),p) basis set and the polarized continuum model (PCM) revealed that stacked conformations became more stable as the polarity of the solvent increases. Rutledge and co-workers have examined the effects of orientation (vertical displacement, angle of rotation, horizontal displacement, and tilt angle) on the interaction between four aromatic residues (histidine, phenylalanine, tyrosine, and tryptophan) with adenine or 3-methyladenine.[15] Their MP2/aug-cc-pVXZ (X = D,T) calculations show that the relative orientation of stacking interactions within active sites account for 65−75% of the maximum stacking energy. In another study, Rutledge, Campbell-Verduyn, and Wetmore have computed energies of

* To whom all correspondence should be addressed. E-mail: tschumpr@olemiss.edu.
[†] University of Mississippi.
[‡] Murray State University.

10.1021/jp805528v CCC: $40.75
Published on Web 10/16/2008

dimers of four amino acids (histidine, phenylalanine, tyrosine, and tryptophan) and DNA or RNA nucleobases (adenine, cytosine, guanine, thymine, and uracil).[20] From the MP2/6-31G*(0.25) potential energy surfaces examined, large stacking interactions (to a little over -10 kcal mol^{-1}) were found as a function of vertical separation, angle of rotation, and horizontal displacement.

Because the presence of nitrogen atoms in π-stacking interactions has substantial effects on the binding energy,[25,37] it is imperative that the high-accuracy computational procedures applied to the $(C_6H_6)_2$ prototype be extended to more biologically relevant models. Although $(C_6H_6)_2$ and other heterocyclic model systems have been well studied, they are not appropriate in a rigorous investigation of the energetic aspects of π-stacking interactions between the adenine ring and aromatic amino acid side chains such as Phe. The adenine/Phe interaction has been identified in protein complexes vital to many cellular processes. Therefore, specific adenine/Phe model systems have been derived from these protein complexes in order to study the energetic contributions these stacking interactions make to protein−ligand complex formation and ultimately protein action and function.

In the present study, 26 toluene/adenine and toluene/N9-methyladenine (9MeA) dimer models have been generated from crystal structures of adenylate−binding protein complexes that exhibit a π-stacking interaction between a Phe residue and the adenine-bearing ligand. Although previous studies of this nature have acknowledged the importance of basis set incompleteness and higher-order correlation effects,[15,20,28,30] this work is, to our knowledge, the first to directly address both issues and provide reliable estimates of the CCSD(T) complete basis set (CBS) limit for π-stacking interaction energies associated with this important class of protein/adenine interactions.

2. Theoretical Methods

To identify π-stacking interactions between the side chain of Phe and the adenine ring, the Protein Data Bank (PDB), housed at The Research Collaboratory for Structural Bioinformatics,[38,39] was searched using ReliBase,[40] a program designed to identify protein−ligand complexes using specific keywords and criterion.[41] In order to obtain target Phe/adenine stacking interactions, protein complexes containing an adenine ring ligand were first identified. Search terms included words such as adenine, adenosine, and adenosine triphosphate. A total of 281 protein complexes fit this initial criterion. Further analysis was done using Protein Explorer.[42,43] A protein complex was then selected for the present study if it contained a Phe residue in the vicinity of the adenine ring. The final criteria required the phenyl ring of Phe and the adenine ring be to roughly parallel to each other (cf. first paragraph of Results and Discussion) and have a intermolecular distance of 4 Å or less. Ultimately, 26 protein complexes that met the defined parameters were chosen for further study. Their PDB codes are as follows: 1A8P, 1ADY, 1ASZ, 1B76, 1B7Y, 1C0A, 1DGK, 1DQA, 1E22, 1EQ2, 1EVL, 1F2U, 1F52, 1FVI, 1FW6, 1GGM, 1H7X, 1IVH, 1KMN, 1NDP, 1QHA, 1SES, 1ZID, 2PUB, 3KAR, and 8GPB.

Toluene/9MeA and toluene/adenine models of these 26 protein/adenine-bearing ligand complexes were generated by removing all extraneous atoms from the PDB coordinate file (i.e., retaining only the atoms of the interacting rings). Hydrogen atoms were then added to fill the resulting open valences, producing toluene from the Phe side chains and 9MeA from the ligands (or just adenine in the case of 2PUB where adenine is the ligand).

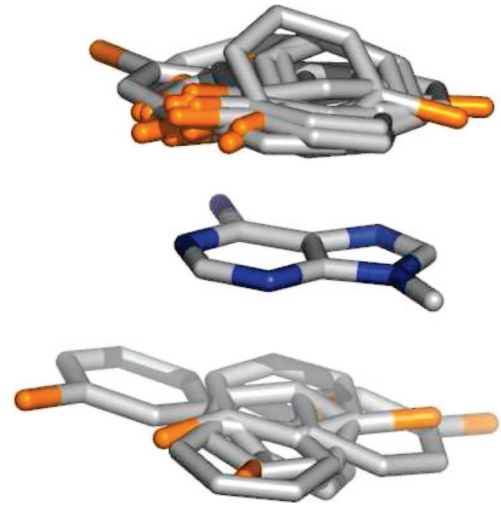

Figure 1. Overlay of the 26 crystal structures for the toluene/9MeA(adenine) model complexes. The β-carbon of Phe is orange, and H atoms are not shown.

Restricting all other atoms, the hydrogen atoms were optimized with molecular mechanics calculations utilizing the Merck Molecular Force Field (MMFF)[44] in the Spartan'04 software package.[45] The convergence criterion for the rms gradient was 4.5×10^{-4} hartree bohr^{-1}, which gave an energy change of 8.0×10^{-5} hartree. The resulting structures have all non-hydrogen atoms in the exact geometry as found in the crystal structure of its original protein complex and are, hereafter, referred to as the "crystal structures". These 26 model systems were then superimposed at the adenine ring to depict the distribution of Phe side chains around this point of reference. The overlay of the 26 crystal structures is shown in Figure 1.

Full geometry optimizations of the 26 crystal structures were initially carried out with the MMFF as described in the previous paragraph. The resulting crystal structures were further refined with second-order Møller−Plesset perturbation theory (MP2) optimizations employing an STO-3G basis set augmented with even-tempered diffuse functions[11,46] on all atoms (α_s(H) = 0.038 228 041, α_{sp}(C) = 0.061 975 480, α_{sp}(N) = 0.079 658 541). This custom basis set is denoted STO-3G++.

After the MMFF and MP2/STO-3G++ optimizations, the 26 toluene/9MeA(adenine) pairs (shown in Figure 1) collapsed to just eight unique structures. These eight structures were then reoptimized at the MP2 level with a double-ζ basis set including diffuse and polarization functions on all atoms (DZP++)[46−48] and only six unique structures remained after optimization at the MP2/DZP++ level. They are shown in Figure 2 and will be referred to as the "optimized structures" in the remainder of this paper. To validate this MP2/STO-3G → MP2/DZP++ optimization procedure, full MP2/DZP++ optimizations were performed on six different structures (1ADY, 1F52, 1FVI, 2PUB, 3KAR, and 8GPB). In each case, both procedures yielded the same optimized structure as long as the same internal coordinates were used.

CCSD(T) complete basis set (CBS) limits of the interaction energy (E_{int}) were estimated for the 26 crystal structures and 6 optimized toluene/9MeA(adenine) dimers using the popular prescription that combines MP2 CBS limit interaction energies with a correction for higher-order correlation effects.[17,18,49−51] MP2 CBS limit values for E_{int} were obtained using the complementary auxiliary basis set explicitly correlated MP2 method (CABS+MP2-R12)[52] implemented in the MPQC software package.[53] The CABS+MP2-R12 calculations employed

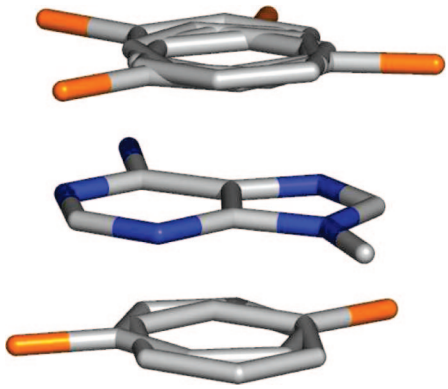

Figure 2. Overlay of the six unique MP2/DZP++ optimized toluene/9MeA(adenine) structures. The β-carbon of Phe is orange, and H atoms are not shown.

the A′ resolution of the identity approximations.[52] A correlation consistent double-ζ basis set, denoted haDZ (cc-pVDZ for H and aug-cc-pVDZ for C and N), was used for the valence basis set while the large K2− − basis set[52,54] was used for the auxiliary basis set. The K2− − basis set is obtained from the K2 basis set[54] by removing basis functions of the two highest orbital angular quantum numbers from each atom.[52] Explicitly correlated R12 methods "bypass the slow convergence of conventional methods, by augmenting the traditional orbital expansions with a small number of terms that depend explicitly on the interelectronic distance $r12$"[55] and, thereby, effectively provide CBS limit correlation energies from a single calculation rather than relying on extrapolation techniques for correlation consistent basis sets. To account for basis set superposition error (BSSE),[56] a standard Boys and Bernardi counterpoise (CP) correction[57,58] was applied to all CABS+MP2-R12 interaction energies. To determine the contribution from higher-order correlation effects, CCSD(T) calculations were performed with the 6-31G*(0.25) basis set.[32] A correction for higher-order correlation effects ($\delta E_{\mathrm{MP2}}^{\mathrm{CCSD(T)}}$) was obtained by taking the difference between the MP2 and CCSD(T) interaction energies without applying CP corrections because it has been shown that they are not needed to obtain reliable $\delta E_{\mathrm{MP2}}^{\mathrm{CCSD(T)}}$ values.[25]

$$E_{\mathrm{int}}^{\mathrm{CCSD(T)/CBS}} = E_{\mathrm{int}}^{\mathrm{MP2/CBS}} + \delta E_{\mathrm{MP2}}^{\mathrm{CCSD(T)}} \qquad (1)$$

The frozen-core approximation was adopted for all computations. Calculations were performed with the MPQC,[53] Molpro,[59] and PSI3[60] quantum chemistry software packages.

3. Results and Discussion

Twenty-six toluene/9MeA(adenine) models of the π-stacking interaction between phenylalanine and adenine-bearing ligands have been generated from PDB crystal structures (Figure 1). After full geometry optimization, these 26 crystal structures collapsed to six distinct geometrical arrangements (Figure 2). The distance (R in angstroms) between the toluene center-of-mass and the 9MeA (or adenine) center-of-mass is reported for each structure in Tables 1 and 2. The angles (in degrees) between the adenine and toluene rings are also reported in Tables 1 and 2. The N-1, C-2, and N-3 atoms define the plane of the adenine ring while C-1, C-2, and C-6 define the toluene plane. When other sets of atoms are used to define the planes, the resulting angles differ only slightly (<1°) from those reported here.

The MP2 and CCSD(T) CBS limit interaction energies of the 26 crystal structures are reported in Table 1. The MP2 E_{int} values are quite large, ranging from −4.78 kcal mol^{-1} for 1FW6 to −9.86 kcal mol^{-1} for 1C0A with an average of −7.32 kcal mol^{-1}. Of course, the MP2 method overestimates E_{int} for π-stacking. The $\delta E_{\mathrm{MP2}}^{\mathrm{CCSD(T)}}$ term in Table 1 corrects for this by accounting for higher-order correlation effects. Despite the fact that the magnitude of this term decreases rapidly as the fragments are separated ($\approx 1/R^6$),[13] the $\delta E_{\mathrm{MP2}}^{\mathrm{CCSD(T)}}$ values for the 26 crystal structures are as large as +3.68 kcal mol^{-1} and average +2.31 kcal mol^{-1}. Combining the two terms yields CCSD(T) CBS limit interaction energies that range from −3.19 to −6.77 kcal mol^{-1} with an average of −5.01 kcal mol^{-1}. The

TABLE 1: Intermolecular Distances (in Å), Angles (in deg), and CBS Limit Interaction Energies (in kcal mol^{-1}) of the 26 Crystal Toluene/9MeA(Adenine) Structures

structure	R^a	θ^b	$E_{\mathrm{int}}^{\mathrm{MP2/CBS}}$	$\delta E_{\mathrm{MP2}}^{\mathrm{CCSD(T)}}$	$E_{\mathrm{int}}^{\mathrm{CCSD(T)/CBS}}$
1A8P	3.68	8.3	−7.34	+2.23	−5.12
1ADY	3.88	3.2	−7.50	+2.08	−5.43
1ASZ	3.75	4.6	−8.58	+2.84	−5.75
1B76	3.90	27.4	−6.65	+2.47	−4.18
1B7Y	3.88	5.5	−7.87	+2.72	−5.15
1C0A	3.45	6.2	−9.86	+3.68	−6.18
1DGK	3.92	26.4	−6.38	+1.66	−4.71
1DQA	3.97	12.8	−7.09	+2.31	−4.78
1E22	3.53	0.9	−9.75	+2.98	−6.77
1EQ2	3.88	3.6	−7.71	+2.38	−5.33
1EVL	3.87	10.4	−7.72	+2.35	−5.36
1F2U	4.31	16.1	−6.46	+2.01	−4.45
1F52	4.15	34.8	−4.99	+1.28	−3.70
1FVI	4.72	7.40	−5.41	+1.58	−3.83
1FW6	5.02	11.4	−4.78	+1.58	−3.19
1GGM	3.82	8.2	−8.37	+2.92	−5.45
1H7X	3.66	7.9	−8.53	+2.58	−5.95
1IVH	4.63	20.8	−4.86	+1.27	−3.59
1KMN	3.52	13.3	−7.65	+2.86	−4.79
1NDP	3.76	6.9	−6.97	+2.07	−4.91
1QHA	3.92	23.0	−6.40	+1.62	−4.79
1SES	3.80	13.4	−8.27	+2.41	−5.86
1ZID	4.04	29.2	−6.22	+1.63	−4.58
3KAR	3.56	16.2	−8.09	+2.76	−5.33
8GPB	3.58	2.3	−8.87	+2.78	−6.09
2PUB	3.40	11.4	−7.91	+2.95	−4.96
Max	5.02	34.8	−9.86	+3.68	−6.77
Min	3.40	0.9	−4.78	+1.27	−3.19
Avg	3.91	12.8	−7.32	+2.31	−5.01

[a] Distance between toluene and 9MeA (or adenine in the case of 2PUB) centers of mass. [b] Angle between toluene and 9MeA (or adenine in the case of 2PUB) ring planes.

TABLE 2: Intermolecular Distances (in Å), Angles (in deg), and CBS Limit Interaction Energies (in kcal mol^{-1}) of the Six Optimized Toluene/9MeA(Adenine) Structures

structure	R^a	θ^b	$E_{\mathrm{int}}^{\mathrm{MP2/CBS}}$	$\delta E_{\mathrm{MP2}}^{\mathrm{CCSD(T)}}$	$E_{\mathrm{int}}^{\mathrm{CCSD(T)/CBS}}$
opt4[c]	3.25	3.0	−11.10	+4.52	−6.57
opt2[d]	3.37	0.7	−11.38	+4.60	−6.78
opt17[e]	3.29	2.2	−11.28	+4.59	−6.70
opt1-1F52	3.26	2.3	−10.73	+4.50	−6.24
opt1-8GPB	3.22	3.8	−11.56	+4.51	−7.05
opt1-2PUB	3.28	1.2	−10.20	+4.27	−5.93
max	3.37	3.8	−11.56	+4.60	−7.05
min	3.22	0.7	−10.20	+4.27	−5.93
avg	3.28	2.2	−11.04	+4.50	−6.54

[a] Distance between toluene and 9MeA (or adenine in the case of 2PUB) centers of mass. [b] Angle between toluene and 9MeA (or adenine in the case of 2PUB) ring planes. [c] 1A8P, 1F2U, 1H7X, and 3KAR optimized to this structure. [d] 1EQ2 and 1FVI optimized to this structure. [e] 1ADY, 1ASZ, 1B76, 1B7Y, 1C0A, 1DGK, 1DQA, 1E22, 1EVL, 1FW6, 1GGM, 1IVH, 1KMN, 1NDP, 1SES, 1QHA, and 1ZID optimized to this structure.

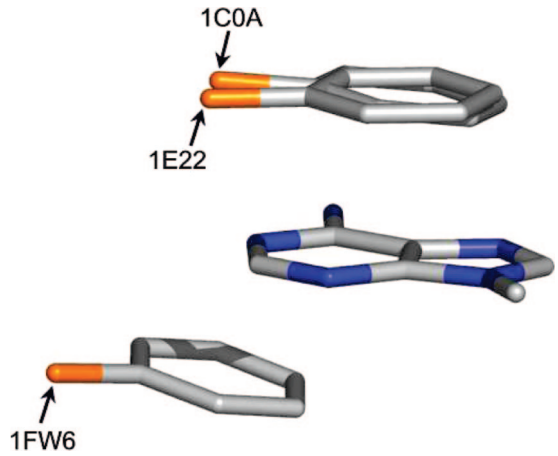

Figure 3. Overlay of the most and least stable crystal structures: 1C0A most stable at MP2 CBS limit, 1E22 most stable at CCSD(T) CBS limit, and 1FW6 least stable at MP2 and CCSD(T) CBS limits. The β-carbon of Phe is orange, and H atoms are not shown.

importance of the higher-order correlation effects is evident when computing E_{int} for 1C0A and 1E22. At the MP2 CBS limit, 1C0A is the most stable dimer. At the CCSD(T) CBS limit, however, 1E22 is 0.59 kcal mol^{-1} more stable than 1C0A. In contrast, 1FW6 is the least stable toluene/9MeA(adenine) pair at both the MP2 and CCSD(T) CBS limits. An overlay of the 1C0A, 1E22, and 1FW6 crystal structures is shown in Figure 3.

Interaction energies for the six unique optimized toluene/9MeA(adenine) structures are reported in Table 2. Upon optimization, 17 of the 25 toluene/9MeA models collapse to the same conformation, which is denoted opt17 because 17 of the crystal structures optimized to that geometry. This set of 17 complexes includes the most and least stable crystal structures (1C0A, 1E22, and 1FW6 in Table 1). Similar nomenclature was adopted for the other optimized structures.[61] PDB codes were appended to the opt1 labels to avoid ambiguity. The most stable optimized toluene/9MeA structure (opt1-8GPB in Table 2) has an interaction energy of -7.05 kcal mol^{-1} at the CCSD(T) CBS limit and was obtained by applying the geometry optimization procedures described in section 2 to the 8GPB crystal structure. No other complex converged to this structure.

As expected, the MP2 CBS limit interaction energies of the optimized complexes in Table 2 are larger than those reported for the crystal structures in Table 1 (by 3.72 kcal mol^{-1} on average). With only six unique optimized structures, the MP2 E_{int} span a fairly narrow range of 1.36 kcal mol^{-1} (from -10.20 to -11.56 kcal mol^{-1}) compared to a range of more than 5 kcal mol^{-1} for the crystal structures. In contrast, the CCSD(T) CBS limit interaction energies increase by only 1.53 kcal mol^{-1} on average when the toluene/9MeA(adenine) dimers are optimized. The average E_{int} at the CCSD(T) CBS limit in Table 2 is -6.54 kcal mol^{-1}. Higher-order correlation effects are responsible for this relatively modest increase from an average of -5.01 kcal mol^{-1} in Table 1. The repulsive $\delta E_{MP2}^{CCSD(T)}$ term increases by more than 2 kcal mol^{-1} on average (to $+4.50$ kcal mol^{-1}) when the structures are optimized, which attenuates the large increases in the interaction energy at the MP2 CBS limit. The $\delta E_{MP2}^{CCSD(T)}$ quantities reported here are appreciably larger than those reported for stacked DNA base pairs in the JSCH-2005 benchmark database[17,62] where $\delta E_{MP2}^{CCSD(T)}$ ranged from $+1.82$ to $+3.57$ kcal mol^{-1} for methylated and non-methylated adenine/thymine and guanine/cytosine dimers when computed with modified cc-pVDZ basis sets.

The CCSD(T) CBS limit interaction energies reported here for these toluene/9MeA(adenine) systems are reasonably consistent with MP2 interaction energies already reported for similar systems. Using benzene/adenine to model the Phe/ligand interactions in six complexes, Mao et al. computed MP2/6-311+G* E_{int} values that ranged from -0.54 to -6.37 kcal mol^{-1}.[30] Two other investigations have probed benzene/adenine interactions with the MP2 method. They report optimal benzene/adenine interaction energies of -5.81 kcal mol^{-1} with the 6-31G*(0.25) basis set[20] and -8.05 kcal mol^{-1} with the aug-cc-pVTZ basis set.[15] Despite similarities between these MP2 results and the CCSD(T) interaction energies reported here, MP2 computations were not able to correctly reproduce the CCSD(T) relative energies of the nonoptimized crystal structures examined in this work.

It is interesting to note that the optimized toluene/adenine complex (opt1-2PUB in Table 2) has a smaller interaction energy than the five optimized toluene/9MeA structures while the E_{int} of the 2PUB crystal structure in Table 1 is very close to the average value for the 25 toluene/9MeA crystal structures. At the CCSD(T) CBS limit, E_{int} of the toluene/adenine complex increases by no more than 1.12 kcal mol^{-1} (from -5.93 to -7.05 kcal mol^{-1}) upon methylation at the N9 position of adenine. In contrast, MP2/aug-cc-pVTZ computations on benzene/adenine complexes indicate that methylation at the N3 position of adenine increases E_{int} by 5.33 kcal mol^{-1} (from -8.05 to -13.38 kcal mol^{-1}), presumably due to the cationic nature of N3-methyladenine.[15]

4. Conclusions

To probe the π-stacking interactions between Phe residues and adenine-bearing ligands, 26 toluene/9MeA(adenine) models have been generated from PDB crystal structures. Full geometry optimizations cause the 26 crystal structures to collapse to six unique MP2/DZP++ optimized structures. Explicitly correlated CABS+MP2-R12 and CCSD(T) computations have been combined to estimate the CBS limit of the CCSD(T) interaction energies for these 32 structures. The CCSD(T) CBS limit interaction energies of the six optimized structures are quite large, ranging from -5.93 to -7.05 kcal mol^{-1} with an average of -6.54 kcal mol^{-1}. These interactions proved to be quite strong in the 26 crystal structures as well where the CCSD(T) CBS limit interaction energy was at least -3.19 kcal mol^{-1} and as large as -6.77 kcal mol^{-1} at the CCSD(T) CBS limit. These values represent $\approx$45%$-$96% (71% on average) of the maximum interaction energy which indicates that π-stacking interactions in complexes involving Phe and an adenine ring are not optimal in terms of geometry/energy.

This investigation of protein/adenylate$-$ligand interactions also demonstrates that higher-order correlation effects are quite important when describing π-stacking interactions in crystal structures. As expected, the difference between MP2 and CCSD(T) interaction energies ($\delta E_{MP2}^{CCSD(T)}$) is quite large for the six optimized structures (up to $+4.60$ and $+4.50$ kcal mol^{-1} on average). However, these higher-order correlation effects are still quite significant for the 26 crystal structures (as large as $+3.68$ and $+2.31$ kcal mol^{-1} on average). As such, a great deal of care must be exercised when examining these interactions with computational schemes that simply rely on the cancelation of higher-order correlation effects and basis set incompleteness errors. These results highlights the need for the continued development of less demanding methods that can accurately describe π-type interactions (e.g., density functional theory with dispersion,[63] spin scaled MP2 methods,[64,65] spin component scaled CCSD,[66] etc.).

Acknowledgment. The authors thank the Mississippi Center for Supercomputing Research for access to their resources. The authors also thank former group members, Dr. Brian W. Hopkins and Adel ElSohly, for their valuable suggestions and helpful discussions. Financial support for this work was provided, in part, to G.S.T. from the National Science Foundation (EPS-0132618, CHE-0517067) and to J.R.C. from the American Chemical Society−Petroleum Research Fund (39739-B).

Supporting Information Available: Cartesian coordinates of the six unique MP2/DZP++ optimized toluene/9MeA(adenine) complexes; MP2 and CCSD(T) interaction energies obtained with the 6-31G*(0.25) basis set. This material is available free of charge via the Internet at http://pubs.acs.org.

References and Notes

(1) McGaughey, G. B.; Gagne, M.; Rappe, A. K. *J. Biol. Chem.* **1998**, *273*, 15458–15463.
(2) Scheiner, S., Ed.; *Molecular Interactions from van der Waals to Strongly Bound Complexes*, 3rd ed.; John Wiley and Sons: Chichester, England, 1997.
(3) Scheraga, H. A., Ed.; *Protein Structure*; Academic Press: New York, 1961.
(4) Šponer, J.; Jurecka, P.; Marchan, I.; Luque, F. J.; Orozco, M.; Hobza, P. *Chem.−Eur. J.* **2006**, *12*, 2854–2865.
(5) Piosik, J.; Zdunek, M.; Kapuscinski, J. *Biochem. Pharmacol.* **2002**, *63*, 635–646.
(6) Chen, R. J.; Bangaruntip, S.; Drouvalakis, K. A.; Kim, N. W. S.; Shim, M.; Li, Y.; Lim, W.; Utz, P. J.; Dai, H. *Proc. Natl. Acad. Sci. U.S.A.* **2003**, *100*, 4984–4989.
(7) Hobza, P.; Selzle, H. L.; Schlag, E. W. *Collect. Czech. Chem. Commun.* **1992**, *57*, 1186–1190.
(8) Hobza, P.; Selzle, H. L.; Schlag, E. W. *J. Phys. Chem.* **1996**, *100*, 18790–18794.
(9) Šponer, J.; Hobza, P. *Chem. Phys. Lett.* **1997**, *267*, 263−270.
(10) Hobza, P.; Šponer, J. *Chem. Rev.* **1999**, *99*, 3247–3276.
(11) Leininger, M. L.; Nielsen, I. M. B.; Colvin, M. E.; Janssen, C. L. *J. Phys. Chem. A* **2002**, *106*, 3850–3854.
(12) Tsuzuki, S.; Honda, K.; Azumi, R. *J. Am. Chem. Soc.* **2002**, *124*, 12200–12209.
(13) Sinnokrot, M. O.; Sherrill, C. D. *J. Phys. Chem. A* **2004**, *108*, 10200–10207.
(14) Waller, M. P.; Robertazzi, A.; Platts, J. A.; Hibbs, D. E.; Williams, P. A. *J. Comput. Chem.* **2006**, *27*, 491–504.
(15) Rutledge, L. R.; Campbell-Verduyn, L. S.; Hunter, K. C.; Wetmore, S. D. *J. Phys. Chem. B* **2006**, *110*, 19652–19663.
(16) Hill, J. G.; Platts, J. A.; Werner, H.-J. *Phys. Chem. Chem. Phys.* **2006**, *8*, 4072–4078.
(17) Jurecka, P.; Šponer, J.; Černý, J.; Hobza, P. *Phys. Chem. Chem. Phys.* **2006**, *8*, 1985–1993.
(18) Sinnokrot, M. O.; Sherrill, C. D. *J. Phys. Chem. A* **2006**, *110*, 10656–10668.
(19) Lee, E. C.; Kim, D.; Jurečka, P.; Tarakeshwar, P.; Hobza, P.; Kim, K. S. *J. Phys. Chem. A* **2007**, *111*, 3446–3457.
(20) Rutledge, L. R.; Campbell-Verduyn, L. S.; Wetmore, S. D. *Chem. Phys. Lett.* **2007**, *444*, 167–175.
(21) Gundersun, S.; Samdal, S.; Strand, T. G.; Volden, H. V. *J. Mol. Struct.* **2007**, *832*, 164–171.
(22) Arnstein, S. A.; Sherrill, C. D. *Phys. Chem. Chem. Phys.* **2008**, *10*, 2646–2655.
(23) Šponer, J.; Riley, K.; Hobza, P. *Phys. Chem. Chem. Phys.* **2008**, *10*, 2595–2610.
(24) Rubes, M.; Bludsky, O. *Phys. Chem. Chem. Phys.* **2008**, *10*, 2611–2615.
(25) Bates, D. M.; Anderson, J. A.; Oloyede, P.; Tschumper, G. S. *Phys. Chem. Chem. Phys.* **2008**, *10*, 2775–2779.
(26) Weck, M.; Dunn, A. R.; Matsumoto, K.; Coates, G. W.; Lobkovsky, E. B.; Grubbs, R. H. *Angew. Chem., Int. Ed.* **1999**, *38*, 2741–2745.
(27) Sinnokrot, M. O.; Valeev, E. F.; Sherrill, C. D. *J. Am. Chem. Soc.* **2002**, *124*, 10887–10893.
(28) Ugozzoli, F.; Massera, C. *CrystEngComm* **2005**, *7*, 121–128.
(29) Chene, P. *Nat. Rev. Drug Discovery* **2002**, *1*, 665–673.
(30) Mao, L.; Wang, Y.; Liu, Y.; Hu, X. *J. Mol. Biol.* **2004**, *336*, 787–807.
(31) Mao, L.; Wang, Y.; Liu, Y.; Hu, X. *J. Am. Chem. Soc.* **2003**, *125*, 14216–14217.
(32) Hobza, P.; Sponer, J.; Polasek, M. *J. Am. Chem. Soc.* **1995**, *117*, 792–798.
(33) Šponer, J.; Leszczynski, J.; Hobza, P. *J. Phys. Chem.* **1996**, *100*, 5590–5596.
(34) Florián, J.; Šponer, J.; Warshel, A. *J. Phys. Chem. B* **1999**, *103*, 884–892.
(35) Jurečka, P.; Šponer, J.; Hobza, P. *J. Phys. Chem. B* **2004**, *108*, 5466–5471.
(36) Cauët, E.; Rooman, M.; Wintjens, R.; Liévin, J.; Biot, C. *J. Chem. Theory Comput.* **2005**, *1*, 472–483.
(37) Itahara, T.; Imaizumi, K. *J. Phys. Chem. B* **2007**, *111*, 2025–2032.
(38) http://www.rcsb.org.
(39) Berman, H. M.; Westbrook, J.; Feng, Z.; Gilliland, G.; Bhat, T. N.; Weissig, H.; Shindyalov, I. N.; Bourne, P. E. *Nucleic Acids Res.* **2000**, *28*, 235–242.
(40) http://relibase.ebi.ac.uk.
(41) Hendlich, M. *Crystallographica D* **1998**, *54*, 1178–1182.
(42) http://www.proteinexplorer.org.
(43) Martz, E. *Trends Biochem. Sci.* **2002**, *27*, 107–109.
(44) Halgren, T. A. *J. Comput. Chem.* **1996**, *17*, 490–519.
(45) Wavefunction, Inc., Irvine, CA, 2004.
(46) Lee, T. J.; Schaefer, H. F. *J. Chem. Phys.* **1985**, *83*, 1784–1794.
(47) Huzinaga, S. *J. Chem. Phys.* **1965**, *42*, 1293–1302.
(48) Dunning, T. H. *J. Chem. Phys.* **1970**, *53*, 2823–2833.
(49) Tsuzuki, S.; Uchimaru, T. *Curr. Org. Chem.* **2006**, *10*, 745–762.
(50) Hobza, P.; Zahradnik, R.; Müller-Dethlefs, K. *Collect. Czech. Chem. Commun.* **2006**, *71*, 443–531.
(51) Tschumper, G. S. Reliable Electronic Structure Computations for Weak Non-Covalent Interactions in Clusters. In *Reviews in Computational Chemistry*; Lipkowitz, K. B., Boyd, D. B., Eds.; VCH, Inc.: New York, Vol. 27, submitted.
(52) Valeev, E. F. *Chem. Phys. Lett.* **2004**, *395*, 190–195.
(53) Colvin, M. E.; Janssen, C. L.; Whiteside, R. A.; Tong, C. H. *Theor. Chim. Acta* **1993**, *84*, 301–314.
(54) Klopper, W. *J. Chem. Phys.* **1995**, *102*, 6168–6179.
(55) Klopper, W.; Manby, F. R.; Ten-No, S.; Valeev, E. F. *Int. Rev. Phys. Chem.* **2006**, *25*, 427–468.
(56) Liu, B.; McLean, A. D. *J. Chem. Phys.* **1973**, *59*, 4557–4558.
(57) Jansen, H. B.; Ros, P. *Chem. Phys. Lett.* **1969**, *3*, 140–143.
(58) Boys, S. F.; Bernardi, F. *Mol. Phys.* **1970**, *19*, 553–566.
(59) Werner, H.-J.; et al. MOLPRO, Cardiff, UK, 2006.
(60) Crawford, T. D.; Sherrill, C. D.; Valeev, E. F.; Fermann, J. T.; King, R. A.; Leininger, M. L.; Brown, S. T.; Janssen, C. L.; Seidl, E. T.; Kenny, J. P.; Allen, W. D. *J. Comput. Chem.* **2007**, *28*, 1610–1616.
(61) Although we have noted that the distribution of optimized structures listed in Table 2 depends on the set of internal coordinates defined by the optimizer and/or the user, the same six structures were obtained even when the distribution changed. Other minima may exist, but those obtained in this work are representative stacked structures for the toluene/9MeA and toluene/adenine systems.
(62) Jurečka, P.; Hobza, P. *J. Am. Chem. Soc.* **2003**, *125*, 15608–15613.
(63) Grimme, S. *J. Comput. Chem.* **2004**, *25*, 1463–1473.
(64) Grimme, S. *J. Chem. Phys.* **2003**, *118*, 9095–9102.
(65) Jung, Y.; Lochan, R. C.; Dutoi, A. D.; Head-Gordon, M. *J. Chem. Phys.* **2004**, *121*, 9793–9802.
(66) Takatani, T.; Hohenstein, E. G.; Sherrill, C. D. *J. Chem. Phys.* **2008**, *128*, 124111.

JP805528V